Journal of Intelligent Material Systems & Structures

Modeling and simulation of the thermo-mechanical response of NiTi based belleville springs

Journal:	*Journal of Intelligent Material Systems and Structures*
Manuscript ID:	Draft
Manuscript Types:	Original Article
Date Submitted by the Author:	n/a
Complete List of Authors:	Sgambitterra, Emanuele; University of Calabria, Department of Mechanical, Energy and Management Engineering Furgiuele, Franco; University of Calabria, Department of Mechanical, Energy and Management Engineering Maletta, Carmine; University of Calabria, Department of Mechanical, Energy and Management Engineering
Keyword:	Shape Memory, NiTi alloys, Belleville, Spring
Abstract:	Nickel-Titanium (NiTi) Belleville washers exhibit unique mechanical and functional features due to the reversible stress induced and/or thermally-induced phase transition mechanism of NiTi alloys. In this paper the thermo-mechanical response of such washers has been analyzed by finite element simulations as well as by a special semi-analytical model, which combines numerical results and analytical methods. The effects of the geometrical configuration of the washers as well as of different thermo-mechanical loading conditions, under stress-induced phase transformation regime, have been analyzed. The results highlighted a marked hysteretic response, in terms of force-deflection curve, due to the hysteresis in the stress-strain behavior of NiTi alloys. In addition, a marked influence of the geometry, as well as of the temperature, has been observed on the thermo-mechanical response of the washer.

Modeling and simulation of the thermo-mechanical response of NiTi based belleville springs

Emanuele Sgambitterra*, Franco Furgiuele and Carmine Maletta
Department of Mechanical, Energy and Management Engineering, University of Calabria, Rende (CS), Italy
*Corresponding author e-mail: esgambitterra@unical.it

Abstract
Nickel-Titanium (NiTi) Belleville washers exhibit unique mechanical and functional features due to the reversible stress induced and/or thermally-induced phase transition mechanism of NiTi alloys. In this paper the thermo-mechanical response of such washers has been analyzed by finite element simulations as well as by a special semi-analytical model, which combines numerical results and analytical methods. The effects of the geometrical configuration of the washers as well as of different thermo-mechanical loading conditions, under stress-induced phase transformation regime, have been analyzed. The results highlighted a marked hysteretic response, in terms of force-deflection curve, due to the hysteresis in the stress-strain behavior of NiTi alloys. In addition, a marked influence of the geometry, as well as of the temperature, has been observed on the thermo-mechanical response of the washer.

Keywords
Shape memory, NiTi alloys, Belleville, spring.

Introduction
Nickel-titanium based (NiTi) shape memory alloys (SMAs) exhibit unique functional features, due to reversible stress induced and/or thermally induced phase transition mechanisms, the so-called shape memory effects (SME) and pseudoelastic effect (PE). In particular, NiTi alloys have the ability to undergo large deformations and to recover their original shape by heating up to a characteristic temperature (SME) or simply by mechanical unloading (PE). Thanks to these unique functional properties coupled with the good mechanical performances and biocompatibility (Otsuka and Ren, 2005), NiTi alloys are currently employed for the realization of smart and/or active components in many fields of engineering and medicine (Otsuka and Wayman, 1998). Despite this technological interest, in last years the use of NiTi alloys has been limited to high-value applications due to the complex material processing and manufacturing. However, the demand for these alloys is rapidly increasing and it is moving from niche markets to mainstream engineering applications, due to a continuous improvement in product quality and reduction in manufacturing costs.
In this context, NiTi alloys are more and more used in several engineering applications, where both SME and PE are exploited for the realization of active and/or tunable components. In particular, SME is mainly used to develop simple actuation systems, which represent efficient and cost effective alternative to complex electromechanical systems (Ikuta et al., 1988; Ikuta, 1990), while PE is largely exploited in the biomedical field, for the realization of several high-value components (e.g. cardiovascular stents, embolic protection filters, micro surgical devices, etc.). However, new applications are arising in last years in mechanical and structural

engineering, where NiTi alloys are used as effective replacements of traditional metallic alloys. In particular, PE coupled with the good mechanical response (*i.e.* large ductility, fatigue resistance, etc.) make NiTi alloys attractive material for structural applications with tunable properties and high damping capabilities (Graesser and Cozzarelli, 1991; Thomson et al., 1995, Dolce and Cardone, 2001, Torra et al., 2010). With this regard, the use of NiTi alloys for the realization of smart springs has been a source of study in the last few years, because they offer very interesting features, such as high recovery capabilities, temperature dependent properties, active and/or tunable response, and high damping properties, thanks to reversible stress-induced martensite (SIM) and/or thermally induced martensite (TIM). The properties of such springs have been exploited for the realization of actuators (Reynaerts and Van Brussel, 1998; Spaggiari et al., 2014), vibration and seismic absorbers (Saadat et al., 2002), orthodontic springs (Wichelhaus et al., 2010), etc. Furthermore, special helical springs with hollow cross section have been also developed (Spinella and Dragoni, 2010; Spinella et al., 2010) with the aim to reduce the heating and cooling time with respect to the solid section. In addition, some research activities have been also devoted to the study of mechanical and functional properties of SMA-based Belleville springs (Labrecque et al., 1996; Speicher et al., 2009; Trochu and Terriault, 1998, Maletta et al. 2013). In particular, the load-deflection curve of a SMA Belleville washer for electrical applications has been numerically analyzed in Trochu and Terriault (1998); the temperature-dependent response of a CuAlNiMnTi-based washer has been analyzed in Labrecque et al. (1996); in Speicher et al. (2009) belleville washers have been used to develop a device for seismic retrofit of buildings, which demonstrated interesting and exploitable damping properties; more recently, numerical simulations and experimental measurements have been carried out in Maletta et. al. (2013) in order to study the influence of the temperature on the thermo-mechanical response of a Belleville washer. In fact, design equations and data for common metallic washers, which are based on theory of elasticity, cannot be directly applied to SMAs due to the complex stress and/or thermally-induced phase transformation mechanisms. As a consequence, continuous developments in the design methodologies should be carried out, concurrently with the advance in material production and processing, to allow effective applicability of SMAs in common engineering fields. Within this context, the present work aims to the development of a simple design method to simulate the thermo-mechanical response of NiTi based washers. In particular, numerical simulations have been carried out, by using a commercial finite element (FE) software code and a special thermo-mechanical constitutive model for SMAs (MSC Marc Theory and User Information, 2007a), in order to analyze the thermo-mechanical behavior of NiTi Belleville springs, in terms of force-deflection response. Subsequently, based on the work by Almen and Laszlo (1936) together with some simplifying assumptions, which arise from a systematic study of the previous numerical results, a semi-analytical model has been developed, which takes into account the phase transition mechanisms in SMAs. The model has been used to analyze the effects of the main geometrical parameters of the washers under different thermo-mechanical loading conditions. In particular, the isothermal mechanical response of Belleville washers, in terms of load-deflection curves for several values of the operating temperature, has been analyzed. The results highlighted that NiTi based Belleville springs exhibit a large hysteretic behavior, as a consequence of the stress-induced phase transition mechanisms, that significantly improve their damping capabilities. Furthermore, the results show that the mechanical and functional

responses of the washers are significantly affected by the operating temperature, as a direct consequence of the thermally-induced microstructural changes.

BELLEVILLE WASHERS: OVERVIEW

Belleville washers are shell annular plates of frusto-conical shape, normally with constant thickness, subjected to axial loads applied along the inner and outer diameter. They are typically made of steel alloy and can be subjected to static and or dynamic loads. Figure 1 illustrates a schematic depiction of a Belleville washer together with the main geometrical parameters, that is, the outer and inner diameters, $2r_o$ and $2r_i$, respectively, the cone height h, and the thickness t. Due to their axial symmetry together with the ability to withstand high mechanical loads with small deflections, Belleville springs are particularly suitable for the realization of modular elastic constructions, where they can be stacked in the same direction, which corresponds to springs in parallel, in an alternating direction, corresponding to springs in series, or in a mixed mode. If compared with more traditional helical springs Belleville washers exhibit a marked nonlinear and/or non-monotonic load-deflection response. Normally, the load versus deflection curves of such springs are given as a function of two non-dimensional geometrical parameters: the ratios h/t and r_o/r_i; the variation of these parameters produces a wide variety of nonlinear load-deflection curves and, in particular, when increasing h/t or decreasing r_o/r_i, a non-monotonic response could be obtained involving a snap-action mechanism. The unusual response of traditional Belleville washers, due to geometric nonlinearities, become even more complex for SMA based washers due to the non-linear hysteretic and temperature dependent stress-strain response of the SMAs, as demonstrated in previous works (Maletta et al., 2013). Three different values of the ratios h/t and r_o/r_i have been considered in the numerical investigation, resulting in a 3x3 factorial design, in order to analyze the effects of the geometry on the whole thermo-mechanical response of the washers, *i.e.* in terms of both mechanical and functional properties. The values of the non-dimensional parameters, illustrated in Table 1, have been chosen based on geometrical dimensions commonly used in machine design (Rothbart and Brown, 1996). Furthermore, the thickness t and the inner radius r_i were held constant, equal to 1.5 mm and 10 mm.

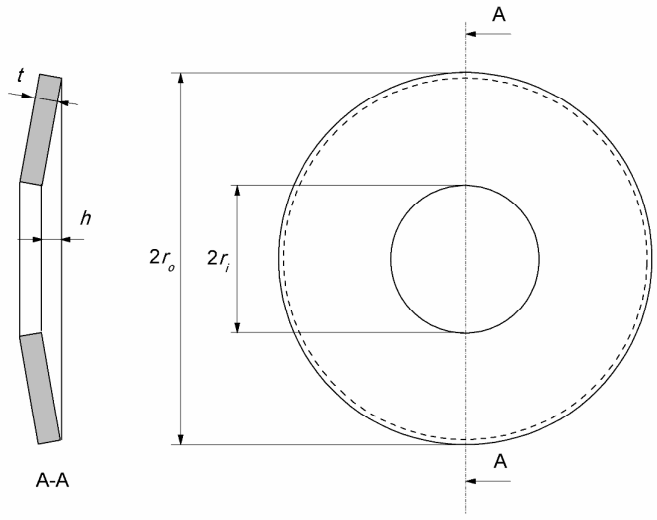

Figure 1. Schematic depiction of a Belleville washer with the main geometrical parameters.

Table 1. Geometrical parameter of the washer

r_o/r_i	h/t
1.75	1
2	1.17
2.25	1.34

NUMERICAL MODELING

The numerical model has been generated by using a commercial finite element software code, that include a special thermo-mechanical constitutive model for shape memory alloys (MSC Marc Theory and User Information, 2007a). In particular 2-D axisymmetric FE models subjected to axisymmetric loads and boundary conditions have been considered for the investigations, as illustrated in Figure 2. In particular, the models have been generated by using about 1500 2D four-node quadrilateral elements and different discretization has been adopted for each combination of the design parameters (h/t and r_o/r_i) based on convergence studies.

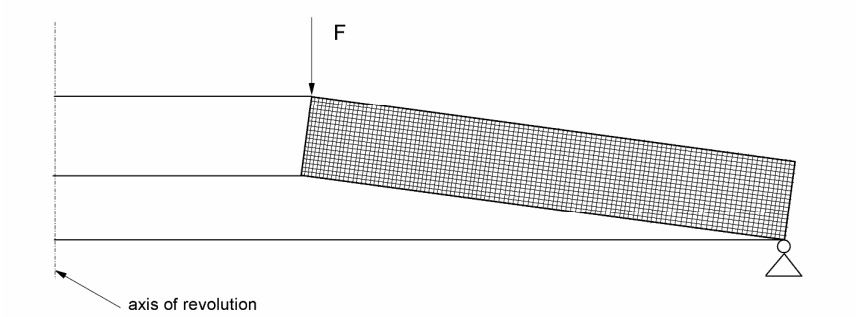

Figure 2. FE model of a cross section of the Belleville spring.

Nonlinear analysis have been carried out by including both geometrical and material nonlinearities. In particular, the model was adopted to overcome some of the limitations of a previous study (Maletta et al., 2013), where a simplified constitutive model for SMAs was used, which does not take into account the mismatch between the Young's modulus of austenite and martensite (E_A and E_M). In particular, the adopted model is based on 16 thermo-mechanical parameters, whose values have been obtained from experimental measurements (Maletta et al., 2013), as illustrated in Table 2. It is worth noting that no yielding phenomena have been considered for the austenite phase and a stress-strain symmetric behavior is assumed between tension and compression. A schematic depiction of the stress–strain curve of the alloy together with the main mechanical parameters is reported in Figure 3.

Special care was devoted to calibrate the constitutive model as well as the iteration parameters of the solver in order to generate an accurate and robust FE models. In fact, an accurate calibration allows to overcome numerical difficulties which normally arise in the unloading path, during reverse stress-induced phase transformation from martensite to austenite. Without describing the complex mathematical formulation of the constitutive model, one of the major issue of the numerical calibration consists in an appropriate definition of the following function:

$$g(\sigma_{eq}) = 1 - exp\left[g_a\left(\frac{\sigma_{eq}}{\sigma_0}\right)^{g_b} + g_c\left(\frac{\sigma_{eq}}{\sigma_0}\right)^{g_d} + g_e\left(\frac{\sigma_{eq}}{\sigma_0}\right)^{g_f}\right] \quad (1)$$

Table 2. Thermo-mechanical parameters of the constitutive model

PROPERTY	VALUE
E_A, Young's modulus of austenite	68 GPa
ν_A, Poisson's ratio of austenite	0.33
α_A, Coefficient of thermal expansion of austenite	10^{-5} °C^{-1}
S_{YA}, Initial yield of austenite	10^{20} MPa
A_s, Austenite start temperature	-8°C
A_f, Austenite finish temperature	13°C
C_A, Austenite slope	5°C/MPa
E_A, Young's modulus of martensite	35 GPa
ν_A, Poisson's ratio of martensite	0.33
α_A, Coefficient of thermal expansion of martensite	10^{-5} °C^{-1}
S_{YA}, Initial yield of martensite	1100 MPa
M_s, Martensite start temperature	-50°C
M_f, Martensite finish temperature	-93°C
C_A, Martensite slope	5 MPa °C^{-1}
ξ, Initial volume fraction of Martensite	0
ε_L, Transfromation strain	0.055

In particular, the function g defines the evolution of the transformation strain as a function of the equivalent von Mises stress (σ_{eq}). The parameters g_i (g_a, g_b, g_c, g_d, g_e, g_f) and σ_0, are obtained from experimental measurements and/or tuned based on a trial and error approach. The numerical simulations have been carried out under isothermal and fully austenitic conditions, *i.e.* for temperatures higher than A_f. In particular, five different values of the temperature (298 K, 308 K, 318 K, 328 K and 338 K) have been considered for each combination of the design parameters (see Table 1), resulting in 9x5 numerical case studies.

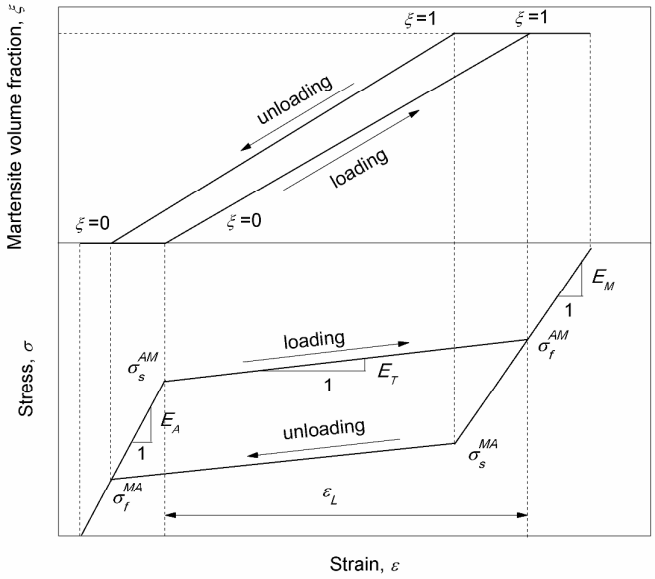

Figure 3. Schematic depiction of the stress–strain curve of the alloy together with the main mechanical parameters.

Preliminary simulations on a pseudoleastic NiTi alloy, with the properties reported in Table 2, have been carried out and the hoop stress distribution (σ_h) in the generic cross section of a Belleville washer has been analyzed (see Figure 4).

If the plasticity concepts are used to define the transformation conditions, similarly to most common numerical models, phase transformation occurs when $\sigma_{eq} \geq \sigma_s^{AM}$, where σ_{eq} represents the equivalent von Mises stress. However, based on the Almen and Laszlo's assumptions, the radial stress component can be neglected and the hoop stress (σ_h) can be directly used as a transformation condition.

Under this assumption, numerical results revealed that for the investigated case studies (see table 1), covering the most typical engineering applications of Belleville washers, the maximum hoop stress, at $r = r_i$, is always lower than the martensite finish stress (σ_f^{AM}), even at the maximum deflection (δ=h), *i.e.* full phase transformation never occurs.

This behavior can be justified analyzing the deformations induced by the applied load. In particular, it can be shown from simple geometrical considerations that the maximum deformation at the inner diameter never reaches the strain value corresponding to the martensite finish stress $\left(\sigma_f^{\mathrm{AM}}\right)$, i.e. $\varepsilon < \left(\sigma_f^{\mathrm{AM}}/E_A + \varepsilon_L\right)$, therefore no one point of the cross section will get full phase transformation.

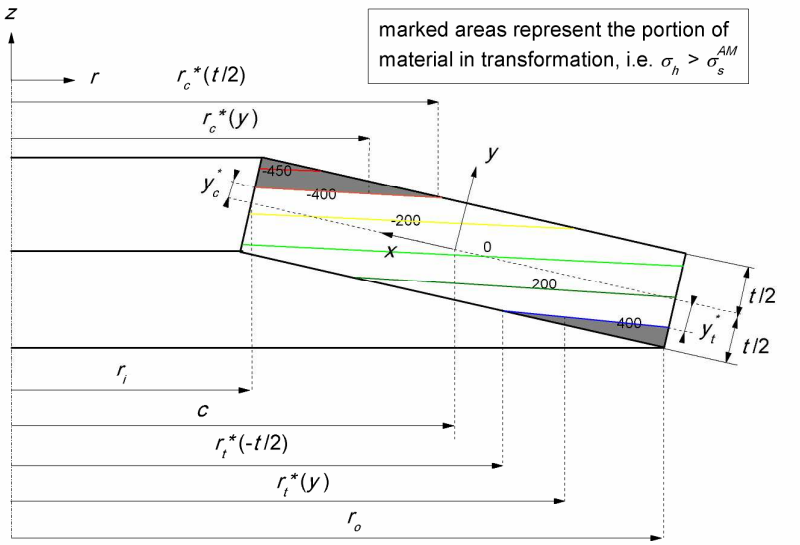

Figure 4. Hoop stress distribution in a generic section of the pseudoelastic Belleville spring. Marked areas represent the portion of material in transformation, i.e. $\sigma_h > \sigma_s^{AM}$.

Furthermore, numerical results revealed that, comparing the elastic and pseudoelastic hoop stress trend along the radius of the washer for a generic y-coordinate (see Figure 5), no significant redistribution due to the martensitic phase transformation occurs in the elastic region of the washer ($\xi = 0$). For the sake of simplicity, Figure 5 refers to the hoop stress distribution at y=t/2, at the maximum deflection (δ=h) and with h/t=1 and r_o/r_i=1.75, but a similar behavior has been observed at a generic y-coordinate in the thickness direction. In particular, the figure reports the hoop stress normalized with respect to the maximum hoop stress at the inner diameter for a linear elastic material ($\sigma_{\mathrm{h\_max}}^{\mathrm{linear}}$).

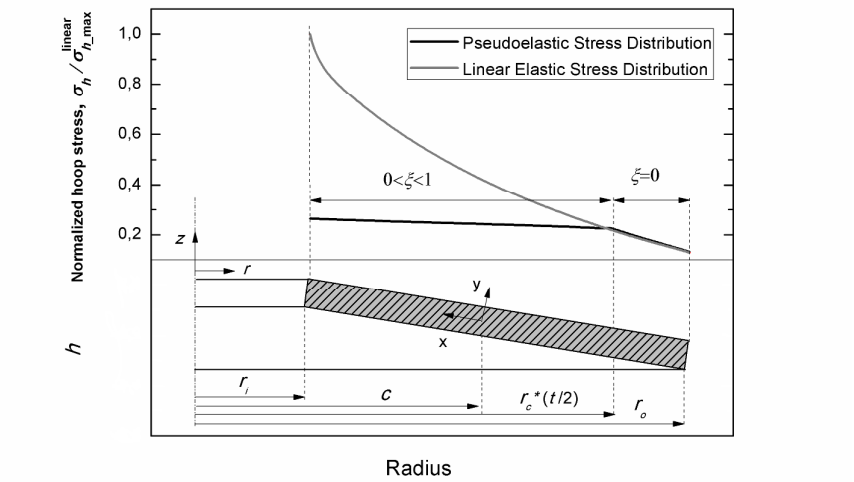

Figure 5. Hoop stress distribution, for the pseudoelastic and elastic material, in a generic section of a Belleville spring at the maximum deflection ($\delta=h$) and $y=t/2$.

ANALYTICAL MODELING

The analytical model to describe the pseusoelastic response of a NiTi Belleville washer has been developed starting from the Almen and Laszlo's work (Almen and Laszlo, 1936). In particular, in this work the non-linear elastic response of a Beleville washer by using the Timoshenko's approach is reported, the radial stress component is neglected, and a rigid rotation of a generic section around a point $c=(r_o-r_i)/ln(r_o/r_i)$ is assumed (see Figure 6).

Results in terms of hoop stress (σ_h), and load (P) as a function of the deflection (δ) are given by the following equations (Almen and Laszlo, 1936):

$$\sigma_h(x,y) = \frac{E\cdot\delta}{(1-\nu^2)(c-x)} \cdot \left[x\left(\beta - \frac{\varphi}{2}\right) + y\right] \tag{2}$$

$$P(\delta) = \frac{E\cdot\delta}{(1-\nu^2)\cdot r_o^2}\left\{\left[\frac{\alpha+1}{\alpha-1} - \frac{2}{log\alpha}\right]\pi\left(\frac{\alpha}{\alpha-1}\right)^2 t(h-\delta)\left(h-\frac{\delta}{2}\right) + \frac{t^3}{6}\pi\cdot log\alpha\left(\frac{\alpha}{\alpha-1}\right)^2\right\} \tag{3}$$

where E is the Young's modulus of the material, ν is the Poisson's ratio, β is the initial angle, φ is the rotation angle, x and y are the components of the local coordinate frame and $\alpha=r_o/r_i$.

Based on the results reported in the previous sections, *i.e.* no full martensitic transformation, no stress redistribution and assuming symmetry between the tensile and compressive stress-strain response of the alloy, the semi-analytical model has been developed.

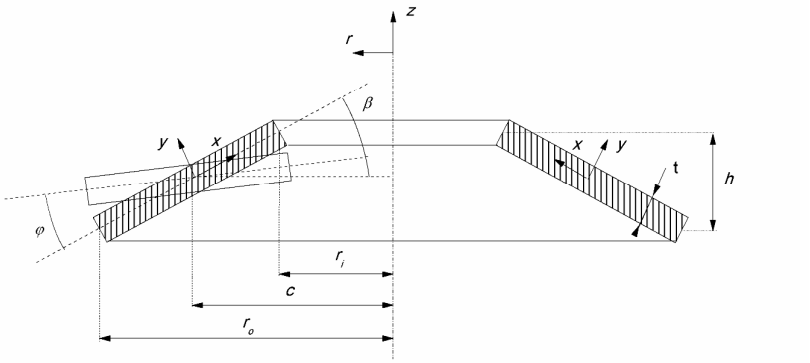

Figure 6. Schematic depiction of a Belleville washer with the main modeling parameters.

The staring point of the model generation is the investigation of the stress distribution, inside the cross section, by means of the following equation:

$$\sigma_h(x,y) = \frac{E_A \cdot \delta}{(1-\nu^2)(c-x)} \cdot \left[x\left(\beta - \frac{\varphi}{2}\right) + y\right] \tag{4}$$

Under the Almen and Laszlo's equation (4) can be directly used as a transformation condition, therefore, when σ_h is lower than the martensite start stress (σ_s^{AM}), no phase transformation occurs, therefore the volume fraction of the martensite is zero (ξ=0). When the stress value is higher than the martensite start stress (σ_s^{AM}), martensitic phase transformation occurs and equation (4) cannot be applied anymore. In fact, due to the generation of the new phase, the effective elastic properties of the material and, consequently, the stiffness of the spring will change.
In order to evaluate the volume fraction of material undergoing phase transformation the simple conditions $\sigma_h(x,y) = \sigma_s^{\mathrm{AM}}$ can be applied in equation (4), which gives the x coordinate where the martensitic transformation starts, namely x^*, as below:

$$x_c^*(y) = \left[-\frac{E_A \cdot \delta}{(1-\nu^2)} \cdot \left(\beta - \frac{\varphi}{2}\right) + \sigma_s^{AM}\right]^{-1} \cdot \left(\sigma_s^{AM} \cdot c + \frac{E_A \cdot \delta}{(1-\nu^2)} \cdot y\right) \tag{5}$$

$$x_t^*(y) = \left[\frac{E_A \cdot \delta}{(1-\nu^2)} \cdot \left(\beta - \frac{\varphi}{2}\right) + \sigma_s^{AM}\right]^{-1} \cdot \left(\sigma_s^{AM} \cdot c - \frac{E_A \cdot \delta}{(1-\nu^2)} \cdot y\right) \tag{6}$$

where subscripts c and t refer to compression and tensile conditions, respectively. The corresponding transformation radius, can be calculated as (see Figure 4):

$$r_c^*(y) = c - x_c^*(y) \cdot \cos(\beta - \varphi) \tag{7}$$

$$r_t^*(y) = c - x_t^*(y) \cdot \cos(\beta - \varphi) \tag{8}$$

For small angles $\cos(\beta\text{-}\varphi)$=1, therefore equations (7) and (8) can be rewritten as:

$$r_c^*(y) = c - x_c^*(y) \tag{9}$$

$$r_t^*(y) = c - x_t^*(y) \tag{10}$$

The integration of equations (9) and (10) along the thickness direction, gives the portion of the cross section undergoing phase transformation as function of the deflection (δ), namely $A^*(\delta)$, as follow:

$$A_c^*(\delta) = \int_{y_c^*}^{+t/2} (r_c^* - r_i)\, dy \tag{11}$$

$$A_t^*(\delta) = \int_{-t/2}^{y_t^*} (r_o - r_t^*)\, dy \tag{12}$$

Where y_c^* and y_t^* are the y-coordinate values corresponding to the transformation condition at $r = r_i$ and $r = r_o$, respectively (see Figure 4). In particular, y_c^* and y_t^* can be directly obtained from equations 9 and 10 by imposing the conditions $r_c^*(y) = r_i$ and $r_t^*(y) = r_o$, respectively:

$$y_c^*(\delta) = -\left(\beta - \frac{\varphi}{2}\right)\left\{r_i \cdot \left[\left[\frac{E_A \cdot \delta}{(1-\nu^2)} \cdot \left(\beta - \frac{\varphi}{2}\right)\right]^{-1} \cdot \sigma_s^{AM} - 1\right] + c\right\} \tag{13}$$

$$y_t^*(\delta) = \left(\beta - \frac{\varphi}{2}\right)\left\{r_o \cdot \left[\left[\frac{E_A \cdot \delta}{(1-\nu^2)} \cdot \left(\beta - \frac{\varphi}{2}\right)\right]^{-1} \cdot \sigma_s^{AM} + 1\right] - c\right\} \tag{14}$$

The volume fraction of material undergoing phase transformation can be calculated, with a good approximation, by the ratio between the area under phase transformation ($A_c^* + A_t^*$) and the total area (A_{tot}) as follow:

$$\bar{A} = \frac{A_c^* + A_t^*}{A_{tot}} \tag{15}$$

It is worth noting that, regardless of the percentage of generated martensite, the material interested by the phase transformation has always a tangent modulus E_T equal to (see Figure 3):

$$E_T = \frac{\sigma_f^{AM} - \sigma_s^{AM}}{\varepsilon_L} \tag{16}$$

Therefore, based on the Timoshenko's assumptions, which neglects the radial stress component (see Figure 7), the effective Young's modulus of the washer, E_e, can be calculated by the mixture law:

$$E_e(\bar{A}) = E_A(1 - \bar{A}) + E_T\bar{A} \tag{17}$$

Substituting the effective Young's modulus in equation (3), it is possible to define the load-deflection response of the pseudoelastic NiTi washer as below:

$$P(\delta) = \frac{E_e \cdot \delta}{(1-\nu^2)\cdot r_o^2}\left\{\left[\frac{\alpha+1}{\alpha-1} - \frac{2}{log\alpha}\right]\pi\left(\frac{\alpha}{\alpha-1}\right)^2 t(h-\delta)\left(h - \frac{\delta}{2}\right) + \frac{t^3}{6}\pi \cdot \log\alpha\left(\frac{\alpha}{\alpha-1}\right)^2\right\} \tag{18}$$

It is worth noting that this equation is able to well predict the load-deflection response of a NiTi Belleville washer only in the loading path and it cannot provide the correct behavior during unloading. Nonetheless, this law can be sufficiently used to correctly design the spring.

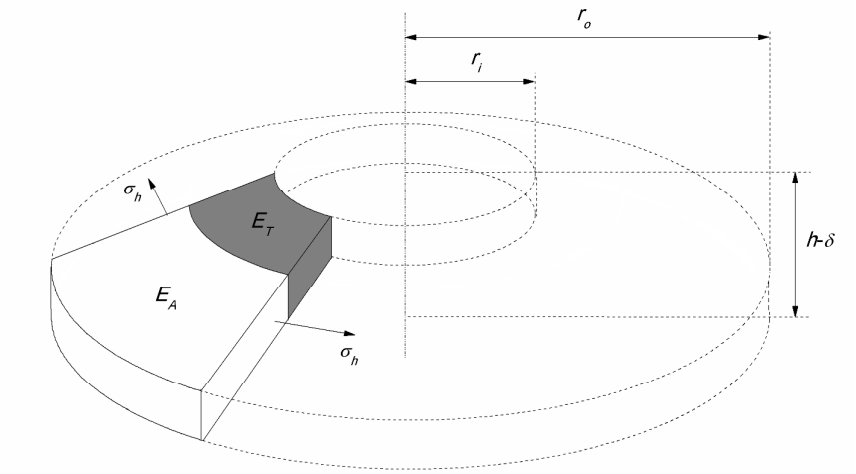

Figure 7. Schematic depiction of the assumption to calculate the effective Young's modulus of the washer.

RESULTS AND DISCUSSION

Results, in terms of load-deflection response, for different testing temperature and geometrical configuration are reported in this section. Based on these results the analytical model has been validated and the effects of both the geometrical configuration of the Belleville washers and of the testing temperature are illustrated and discussed. Figure 8 illustrates a schematic depiction of the load-deflection curve of a NiTi based Belleville washer under pseudoelastic regime, *i.e.* for testing temperatures higher than A_f.

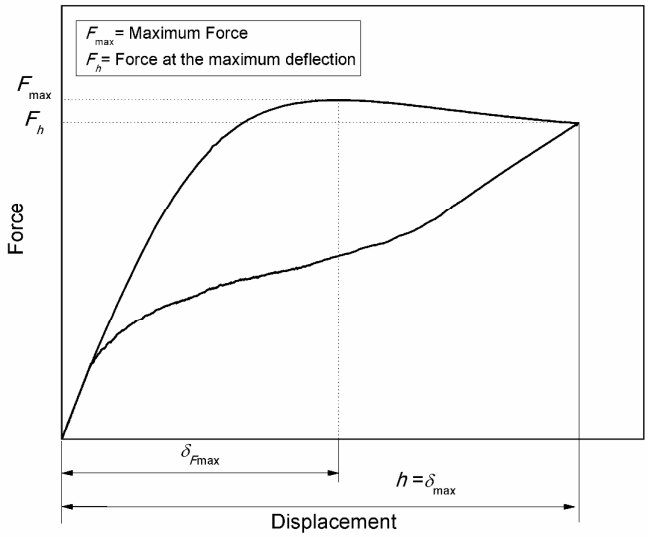

Figure 8. Schematic depiction of the force-deflection curve of a pseudoelastic NiTi based Belleville washer.

The curve represents a typical case of non-monotonic response and it is drawn up to the maximum allowable deflection, equal to the cone height of the washer ($\delta_{max}=h$). In addition, the figure also illustrates the characteristic parameters analyzed in this investigation: the maximum force (F_{max}) and the force at the maximum deflection

(F_h). These two forces are equal ($F_{max}=F_h$) if the washer exhibits a monotonic response.

As observed in Figure 8 as well as in a previous work (Maletta et al., 2013), NiTi based Belleville washers exhibit a marked hysteretic behavior, as a consequence of the hysteresis in the stress-strain response of the material. This is one of the most interesting features of such springs as they provide significant advantages in the field of structural and/or seismic damping, as demonstrated previously (Speicher et al., 2009). In this work, however, the focus was to analytically predict the response during the loading phase; therefore the hysteretic behavior has been only numerically investigated as reported in the next section.

Numerical Investigations

Figure 9 illustrates the numerical isothermal force-deflection curves of a Belleville washer with r_o/r_i=1.75 and h/t=1, for five different values of the temperature (298 *K*, 308 *K*, 318 *K*, 328 *K* and 338 *K*). The figure clearly shows a marked influence of the temperature on both mechanical and functional responses of the washer. In particular, when increasing the temperature, the force-deflection curve approaches the one obtained from a linear elastic material, that is, the transformation mechanism and the hysteretic behavior tend to vanish, as a direct consequence of the increase in the transformation stresses, according to the Clausius-Clapeyron relation.

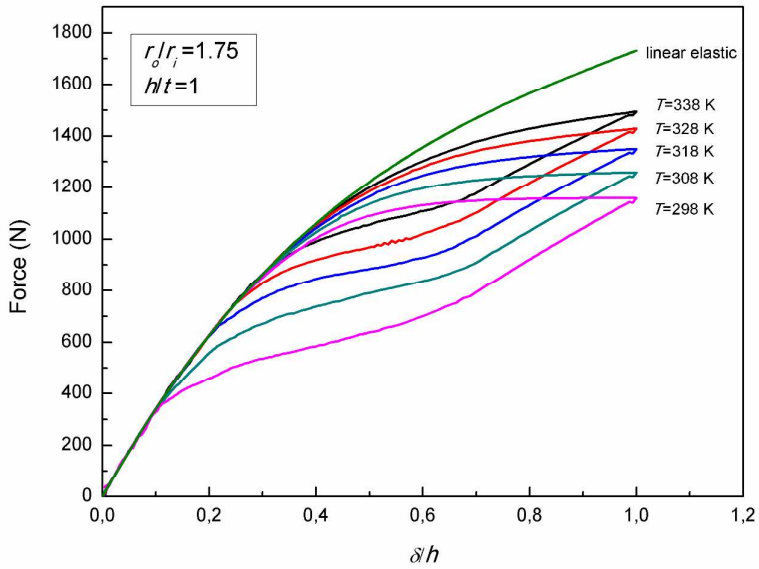

Figure 9. Numerical isothermal force-deflection curves for different values of the temperature for a pseudoelastic NiTi based Belleville washer with r_o/r_i=1.75 and h/t=1. The curve on the top is related to a washer modeled with a linear elastic material.

The effects of the geometrical parameters, r_o/r_i and h/t, on the force-deflection response at room temperature (T=298 *K*) are illustrated in Figures 10 and 11. In particular, Figure 10 shows the effects of the diameter ratio, r_o/r_i, for a fixed value of the cone height ratio h/t=1.17. The figure highlights a marked increase of the stiffness, *i.e.* of the maximum force, as well as of the hysteretic region, *i.e.* of the dissipated energy, with decreasing the r_o/r_i ratio, due to the higher geometric nonlinearities of the washer. These nonlinearities cause high internal stresses generating wide phase transformation zones and resulting in an increase of the hysteretic region. In addition, as a direct consequence of the geometrical

nonlinearities, the curve for r_o/r_i=1.75 shows an evident non-monotonic behavior. Similar considerations can be applied to Figure 11, which illustrates the effects of the height ratio, h/t, for a fixed value of the diameter ratio r_o/r_i=2. In this case, both maximum force and dissipated energy increase with increasing h/t and a marked non-monotonic trend is observed when h/t=1.33.

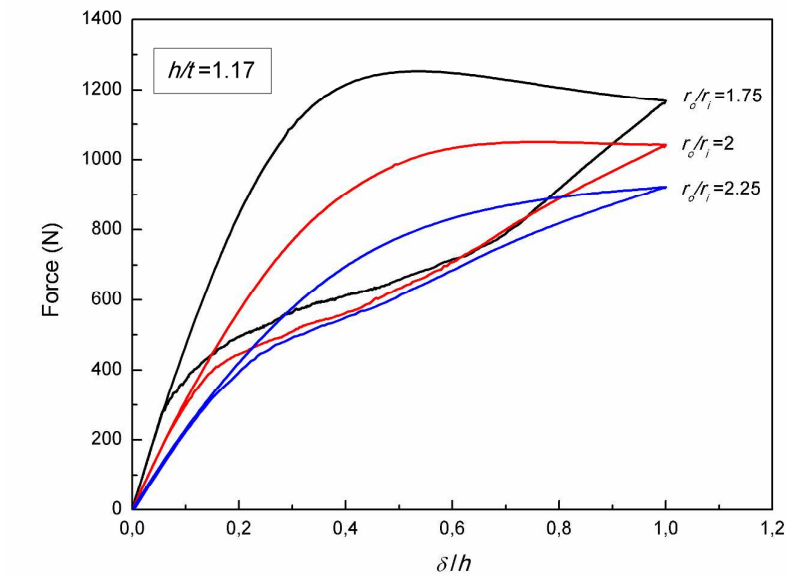

Figure 10. Isothermal force-deflection curves (T=298 K) for a pseudoelastic NiTi based Belleville washer with h/t=1.17 and different values of r_o/r_i.

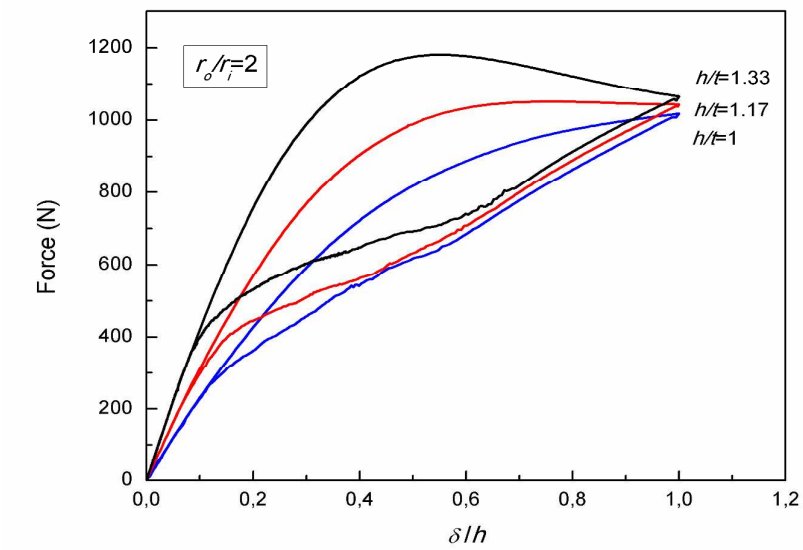

Figure 11. Isothermal force-deflection curves (T=298 K) for a pseudoelastic NiTi based Belleville washer with r_o/r_i =2 and different values of h/t.

Analytical results

Analytical results have been validated by systematic comparisons with the numerical ones as reported in Figures 12-15. In particular, Figures 12 and 13 represent the effect of the operating temperature, for two different geometrical configurations, while in Figures 14 and 15 the effect of the geometry, at room temperature, are illustrated.

All figures clearly show a satisfactory agreement between numerical and analytical results; in particular, it is worth noting that the proposed model is able to well predict the phase transformation mechanism and the trend (monotonic and non-monotonic) of the response in each geometrical configuration and testing temperature.

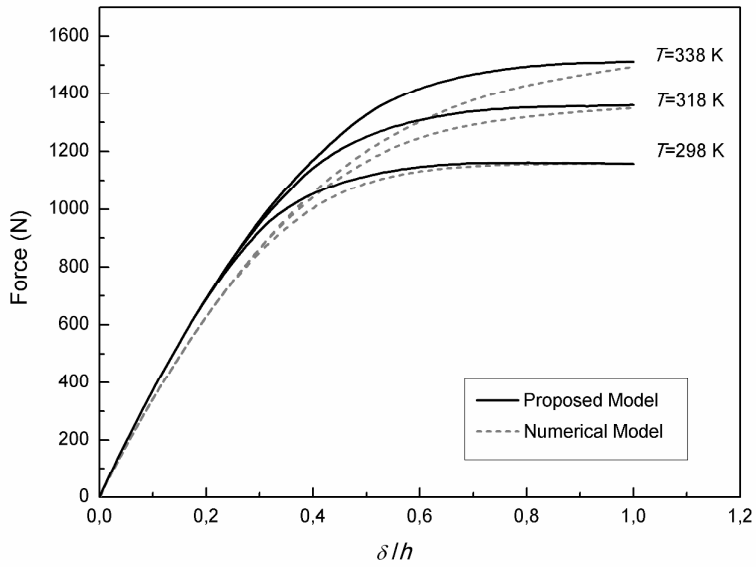

Figure 12. Comparison between the analytical and numerical load-deflection response for a pseudoelastic NiTi based Belleville washer for different testing temperatures. Disk geometry: r_o/r_i=1.75, h/t=1.

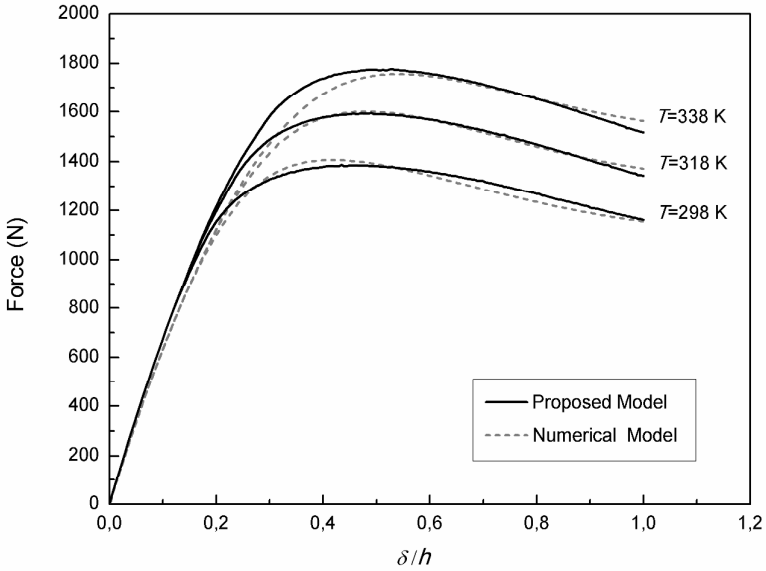

Figure 13. Comparison between the analytical and numerical load-deflection response for a pseudoelastic NiTi based Belleville washer for different testing temperatures. Disk geometry: r_o/r_i=1.75, h/t=1.33.

Results, however, exhibit an higher stiffness in the proposed model with respect to the numerical one, but such behavior is encouraged by a previous comparison between the Almen's model and numerical one on a common engineering material, where a similar behavior was observed (see Figure 16).

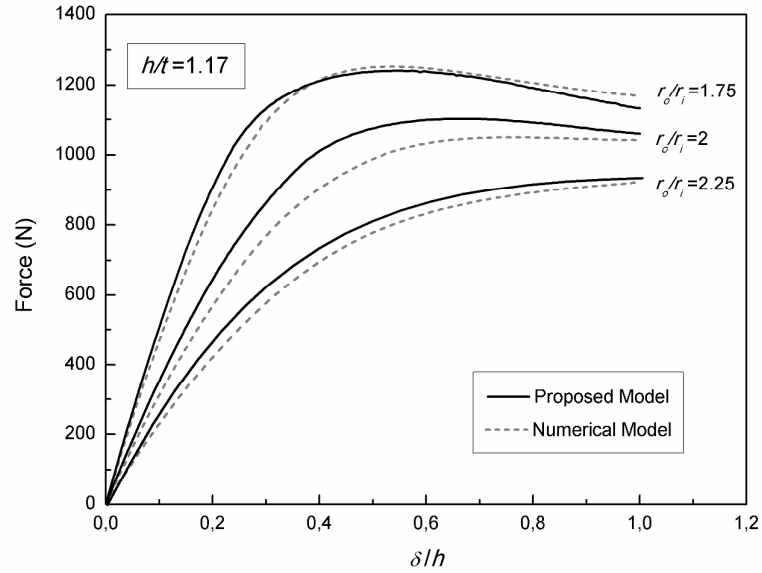

Figura 14. Comparison between the analytical and numerical load-deflection response for a pseudoelastic NiTi based Belleville washer, at room temperature, for different r_o/r_i ratios and h/t=1.17.

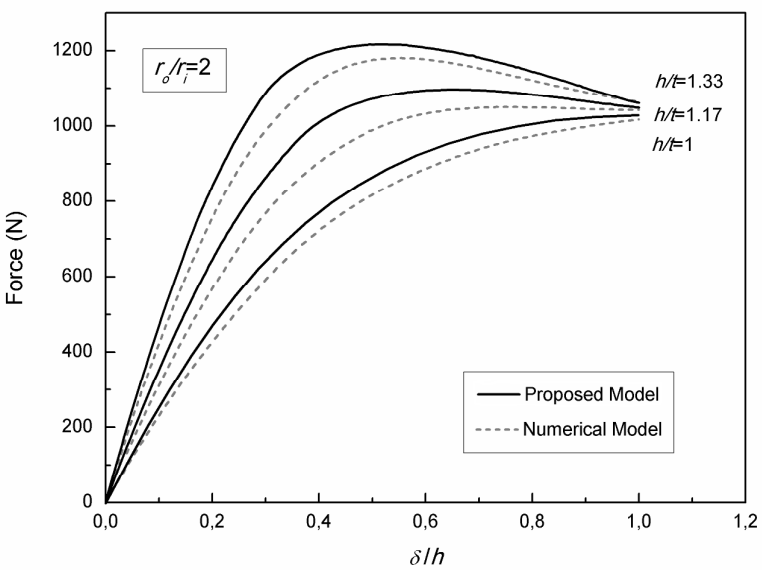

Figura 15. Comparison between the analytical and numerical load-deflection response for a pseudoelastic NiTi based Belleville washer, at room temperature, for different h/t ratios and r_o/r_i =2.

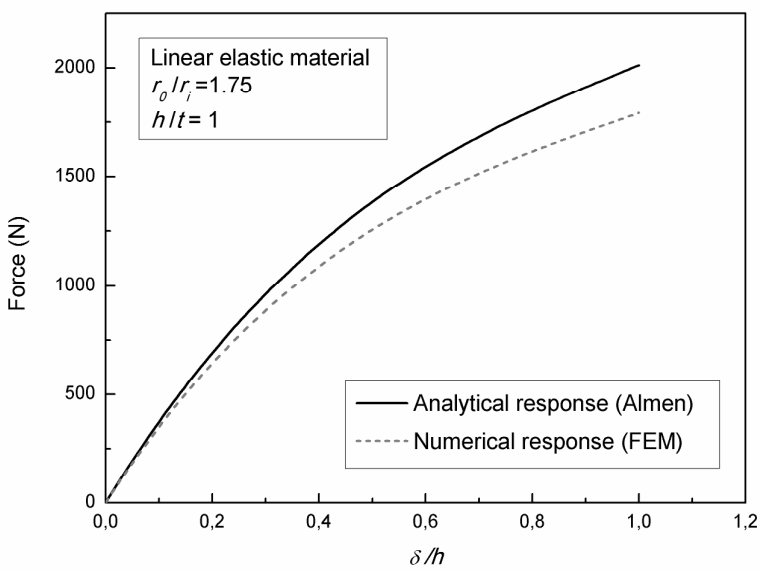

Figure 16. Comparison between the analytical and numerical load-deflection response for a Belleville washer modeled with a linear elastic material, at room temperature. Disk geometry: r_o/r_i=1.75, h/t=1.

Based on these results, the influence of geometrical parameters, *i.e.* the combining effects of r_o/r_i, and h/t, on the mechanical responses of the washers, has been analyzed by means of the proposed model and the results are reported in the 3-D graphs in Figures 17 and 18.

In particular, Figures 17 illustrate the maximum force, F_{max} (Figure 17(a)), and the force at the maximum deflection, F_h (Figure 17(b)), for the lower and upper values of the analyzed temperature (298 K and 338 K). The figures illustrate that both F_{max} and F_h increase with increasing the temperature, which can be directly attributed to the Clausius-Clapeyron effect. Furthermore, both forces increase with increasing h/t and with decreasing r_o/r_i; however the effect of the diameter ratio is more evident than that of the cone height ratio, as also qualitatively shown in Figures 14 and 15.

It is worth noting that most of the engineering applications of Belleville washers normally require monotonic or almost flat force-deflection responses, then the corresponding geometrical configurations, in terms of the ratios h/t and r_o/r_i, should be identified (Speicher et al., 2009). To this aim, Figures 18 illustrate direct comparisons between F_{max} and F_h under isothermal conditions at T=298 K (Figure 18(a)) and at T=338 K (Figure 18(b)). In the figures is easy to identify the geometric domain where the mechanical response of the washer is monotonic, *i.e.* when the maximum force is not greater than the force at the maximum deflection. In addition, a comparison between Figures 18(a) and 18(b) shows that the monotonic geometric domain increases with increasing the operating temperature. This result can be attributed to the increase of the transformation stresses and, consequently, to the reduction of stress-induced phase transition mechanisms.

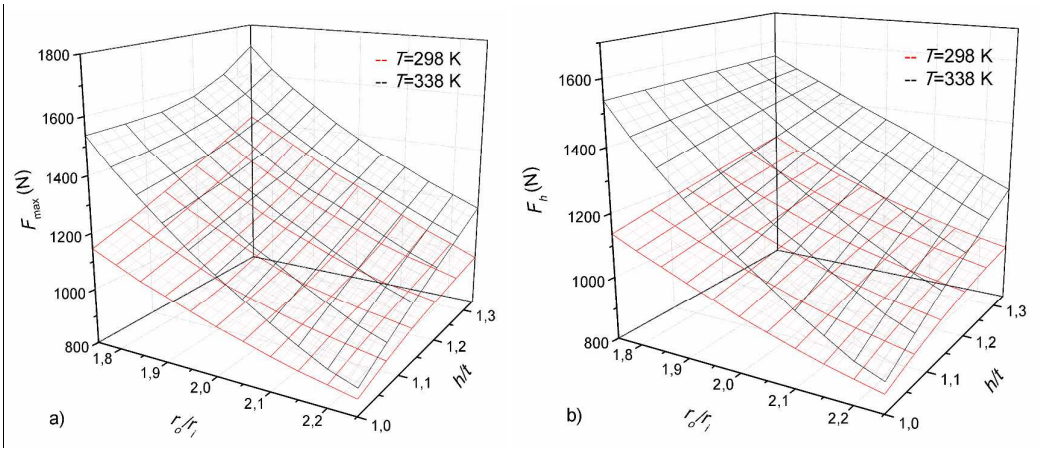

Figure 17. Forces as a function of r_o/r_i and h/t for two different values of the operating temperature (298 K and 338 K): a) maximum force, F_{max}; b) force at the maximum deflection, F_h.

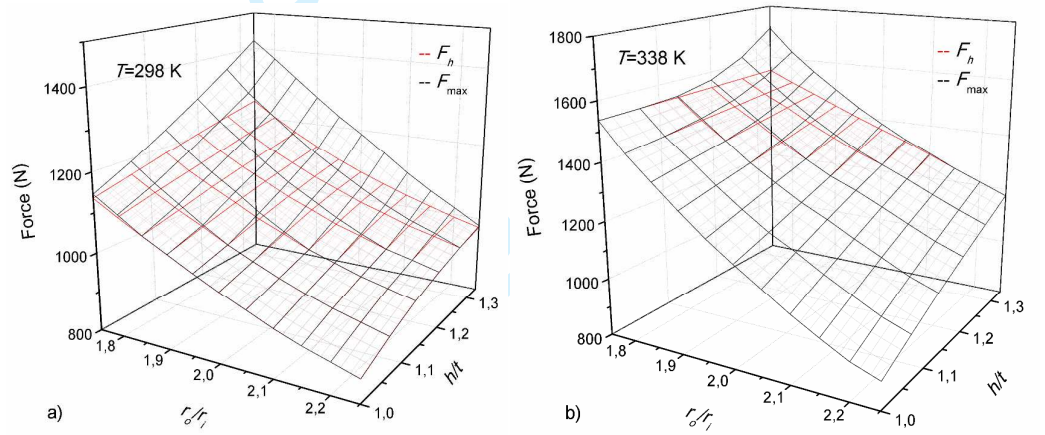

Figure 18. Comparison between the maximum force, F_{max}, and the force at the maximum deflection, F_h, as a function of r_o/r_i and h/t: a) T=298 K; b) T=338 K.

CONCLUSIONS

The thermo-mechanical response of NiTi based Belleville springs have been analyzed by using a commercial FE software code and a special constitutive model for SMAs. Subsequently, based on a systematic analysis of the numerical results some simplifying assumptions have been adopted and a novel and simple analytical model has been developed, which takes into account the martensitic phase transformation in SMAs. The validity of the proposed model has been firstly demonstrated by comparisons with numerical simulations and, subsequently, the model has been used to analyze the effects of the main geometrical parameters, as well as of the operating temperature, on the thermo-mechanical response of the washers.

In particular, two non-dimensional geometrical parameters have been considered: the outer by inner diameter ratio (r_o/r_i) and the cone height by thickness ratio (h/t). The domain of the non-dimensional parameters have been chosen based on geometrical dimensions commonly used in mechanical design. Furthermore, different values of the temperatures, within the fully austenitic regime of the investigated NiTi alloy, have been considered. The results highlighted that NiTi based Belleville washers exhibit unique features with respect the traditional ones, such as a marked temperature

dependent response, due to the variation of the transformation stress with the temperature, according to the Calusius-Clapayron relation. Furthermore, numerical simulations reveled an evident hysteretic behavior, which can be directly attributed to the hysteresis in the stress-strain response of NiTi alloys. The obtained results can be advantageously used for the selection of NiTi-based Belleville washers based on mechanical and/or on functional design needs.

REFERENCES

Almen JO and Laszlo A (1936) The uniform section disk spring. *Transaction of the American Society of Mechanical Engineers*, RP 50-10, pp. 305-314.

Auricchio F and Taylor RL (1997) Shape-memory alloy: modeling and numerical simulations of the finite-strain superelastic behavior. *Computer Methods in Applied Mechanics and Engineering*, Vol. 143, pp. 175–194.

Auricchio F (2001) A robust integration-algorithm for a finite-strain shape memory alloy superelastic mode. *International Journal of Plasticity*, Vol. 17, pp. 971–990.

Dolce M and Cardone D (2001) Mechanical behavior of shape memory alloys for seismic applications 2. Austenite Ni-Ti wires subjected to tension. *International Journal of Mechanical Sciences*, Vol. 43, pp. 2657–2677.

Graesser EJ and Cozzarelli FA (1991) Shape-memory alloys as new materials for aseismic isolation. *Journal of Engineering Mechanics*,Vol. 117, no. 11, pp. 2590–2608.

Ikuta K, Tsukamoto M and Hirose S (1988) Shape Memory Alloy Servo Actuator System with Electric Resistance Feedback and Application for Active Endoscope. *Proceedings- 1988 IEEE International Conference on Robotics and Automation.;Philadelphia, PA, USA*.

Ikuta K (1990) Micro/miniature shape memory alloy actuator. *Proceedings of the 1990 IEEE International Conference on Robotics and Automation;Cincinnati, OH, USA;13-18 May 1990*.

Labrecque C, Braunovic M, Terriault P, Trochu F and Schetky M (1996) Experimental and theoretical evaluation of the behavior of a shape memory alloy Belleville washer under different operating conditions. *Proceedings of the annual Holm conference on electrical contacts, Chicago, IL, 6–20 September 1996,* pp.195–204.

Maletta C, Filice L and Furgiuele F (2013) NiTi Belleville washers: Design, manufacturing and testing. *Journal of Intelligent Material Systems and Structures* 24 (6), pp. 695-703

MSC Marc, Theory and User Information (2007a) Thermo-Mechanical Shape Memory Model. *Vol.. a*, pp. 388-393

Otsuka K and Ren X (2005) Physical metallurgy of Ti-Nibased shape memory alloys. *Progress in Materials Science*, Vol. 50, pp. 511–678.

Otsuka K and Wayman CM (1998) Shape Memory Materials. *Cambridge: Cambridge University Press*.

Reynaerts D and Van Brussel H (1998) Design aspects of shape memory actuators. *Mechatronics*, Vol. 8, pp. 635–656.

Rothbart H and Brown TH (1996) *Mechcanical Design Handbook.* second ed. McGraw Hill.

Saadat S, Salichs J, Noori M, Hou Z, Davoodi H, Bar-on I, Suzuki Y and Masuda A (2002) An overview of vibration and seismic applications of NiTi shape memory alloy. *Smart Materials and Structures*, Vol. 11, pp. 218–229.

Spaggiari A, Dragoni E and Tuissi A (2014) NiTi Alloy Negator Springs for Long-Stroke Constant-Force Shape Memory Actuators: Modeling, Simulation and Testing. *Journal of Materials Engineering and Performance*. DOI: 10.1007/s11665-014-0946-3

Speicher M, Hodgson DE, DesRoches R and Leon RT (2009) Shape memory alloy tension/compression device for seismic retrofit of buildings. *Journal of Materials Engineering and Performance*, Vol. 18(5–6), pp. 746–753.

Spinella I and Dragoni E (2010) Analysis and design of hollow helical springs for shape memory actuators. *Journal of Intelligent Material Systems and Structures*, Vol. 21, 185–199.

Spinella I, Dragoni E and Stortiero F (2010) Modeling, prototyping, nd testing of helical shape memory compression springs with hollow cross section. *Journal of Mechanical Design*, Vol. 132, pp. 1–9.

Thomson P, Balas GJ and Leo PH (1995) The use of shape memory alloys for passive structural damping. *Smart Materials and Structures*, Vol. 4, no. 1, pp. 36–41.

Torra V, Isalgue A, Carreras G, Lovey FC, Soul H, Terriault P and Dieng L (2010) Experimental study of damping in civil engineering structures using smart materials (NiTi - SMA). Application to stayed cables for bridges. *International Review of Mechanical Engineering* 4 (5), pp. 601-611

Trochu F and Terriault P (1998) Nonlinear modelling of hysteretic material laws by dual Kriging and application. *Computer Methods in Applied Mechanics and Engineering*, Vol. 151(3–4), pp. 545–558.

Wichelhaus A, Brauchli L, Ball J and Mertmann M (2010) Mechanical behavior and clinical application of nickeltitanium closed-coil springs under different stress levels and mechanical loading cycles. *American Journal of Orthodontics and Dentofacial Orthopedics*, Vol. 137, pp. 671–678.

Table 1. Geometrical parameter of the washer

r_o/r_i	h/t
1.75	1
2	1.17
2.25	1.34

Table 2. Thermo-mechanical parameters of the constitutive model

PROPERTY	VALUE
E_A, Young's modulus of austenite	68 GPa
ν_A, Poisson's ratio of austenite	0.33
α_A, Coefficient of thermal expansion of austenite	10^{-5} °C^{-1}
S_{YA}, Initial yield of austenite	10^{20} MPa
A_s, Austenite start temperature	-8°C
A_f, Austenite finish temperature	13°C
C_A, Austenite slope	5°C/MPa
E_A, Young's modulus of martensite	35 GPa
ν_A, Poisson's ratio of martensite	0.33
α_A, Coefficient of thermal expansion of martensite	10^{-5} °C^{-1}
S_{YA}, Initial yield of martensite	1100 MPa
M_s, Martensite start temperature	-50°C
M_f, Martensite finish temperature	-93°C
C_A, Martensite slope	5 MPa °C^{-1}
ξ, Initial volume fraction of Martensite	0
ε_L, Transfromation strain	0.055

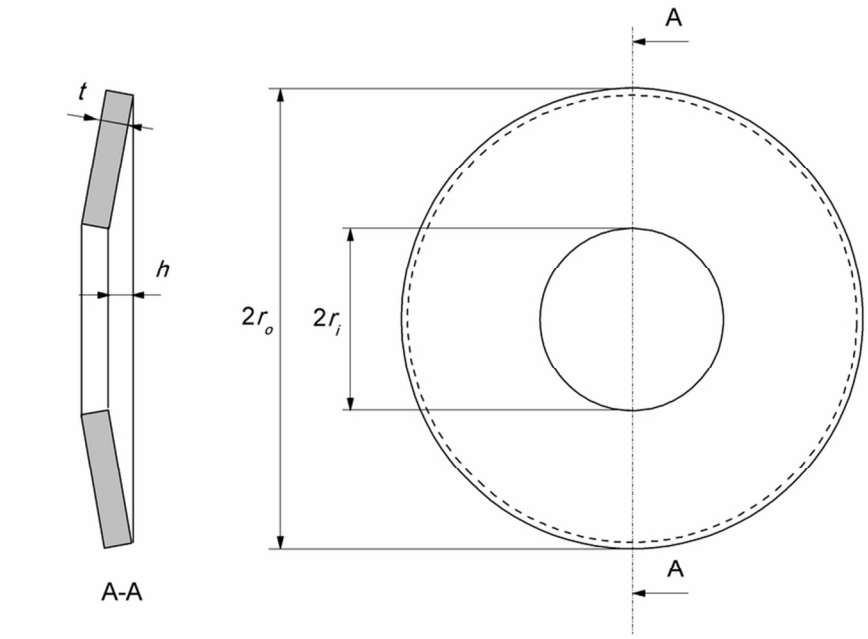

Schematic depiction of a Belleville washer with the main geometrical parameters.
84x58mm (300 x 300 DPI)

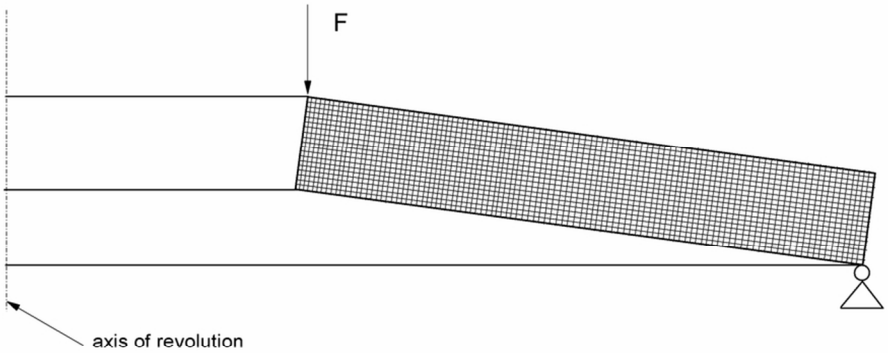

FE model of a cross section of the Belleville spring.
83x58mm (300 x 300 DPI)

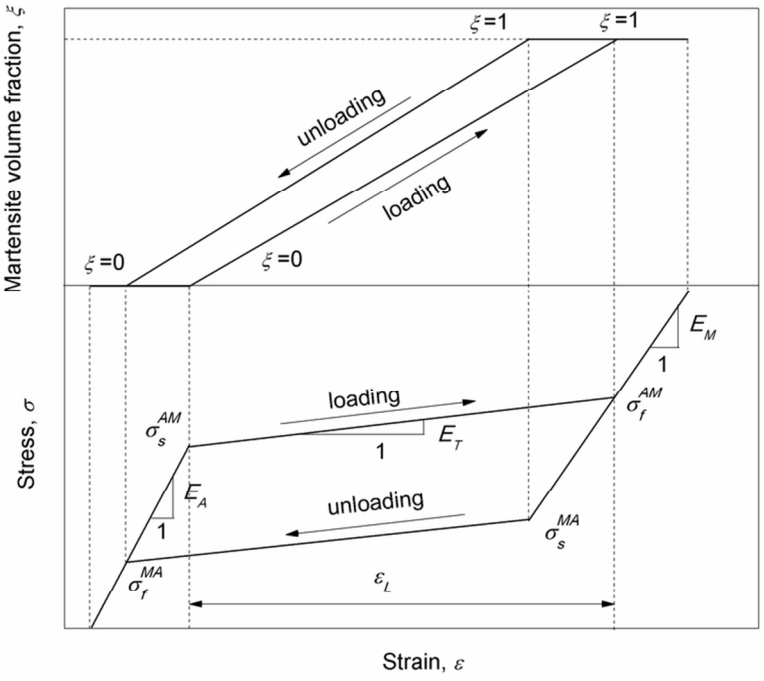

Schematic depiction of the stress–strain curve of the alloy together with the main mechanical parameters.
84x58mm (300 x 300 DPI)

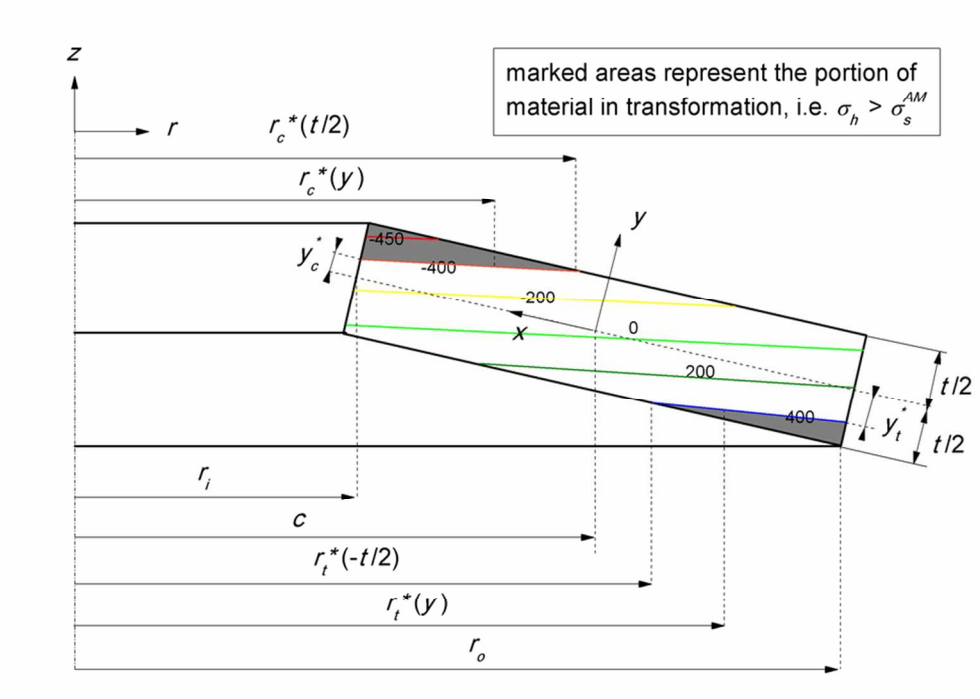

Hoop stress distribution in a generic section of the pseudoelastic Belleville spring. Marked areas represent the portion of material in transformation, i.e. σ_h>σ_s^AM.
84x58mm (300 x 300 DPI)

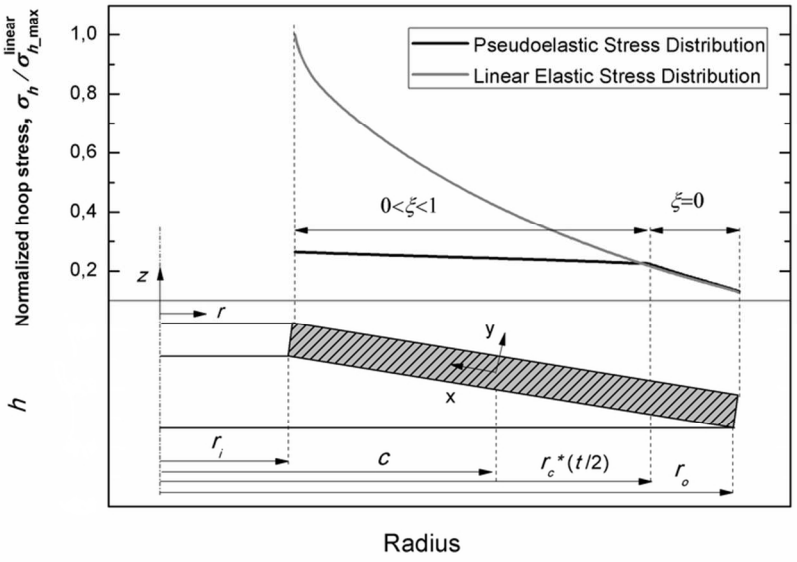

Hoop stress distribution, for the pseudoelastic and elastic material, in a generic section of a Belleville spring at the maximum deflection (δ=h) and y=t/2.
83x58mm (300 x 300 DPI)

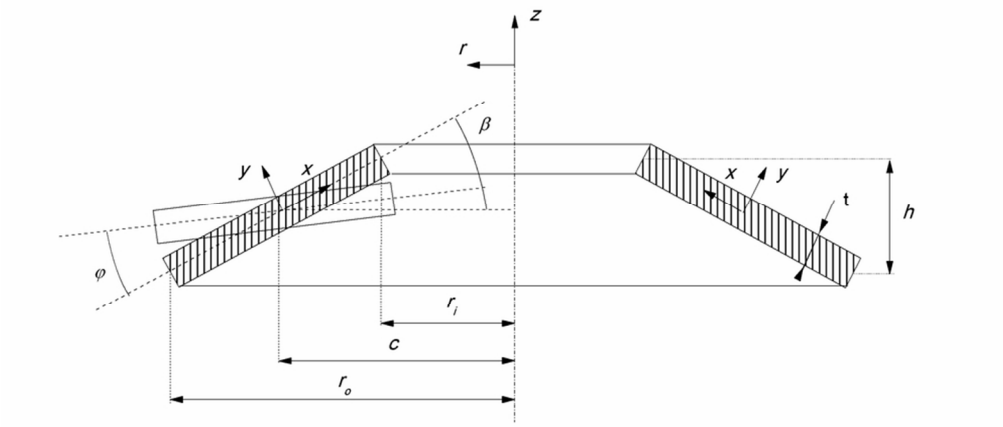

Schematic depiction of a Belleville washer with the main modeling parameters.
84x58mm (300 x 300 DPI)

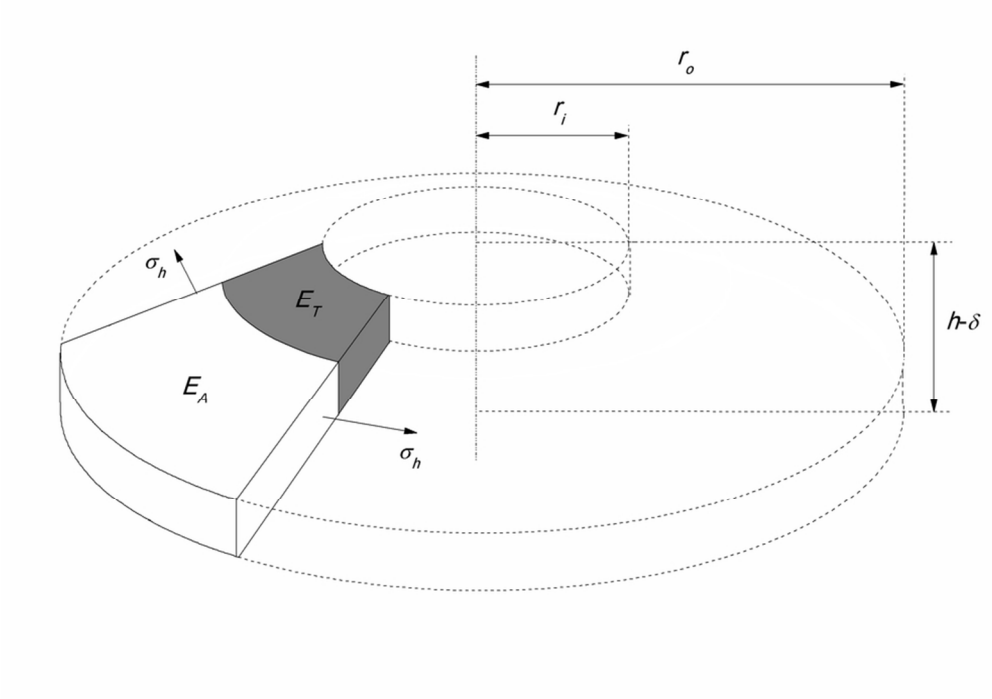

Schematic depiction of the assumption to calculate the effective Young's modulus of the washer.
84x58mm (300 x 300 DPI)

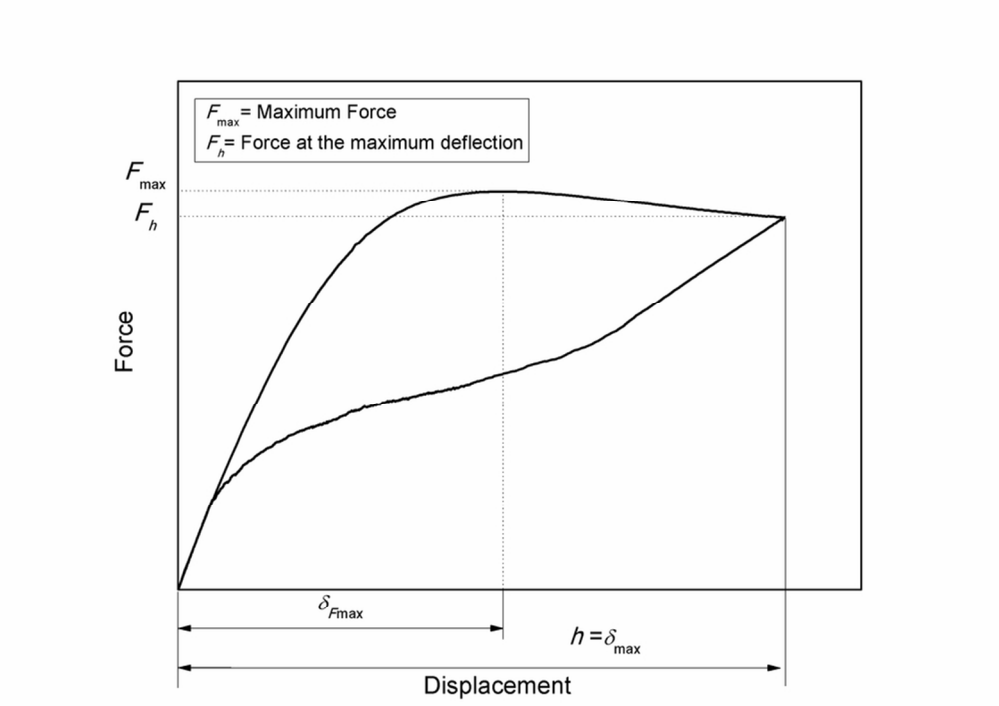

Schematic depiction of the force-deflection curve of a pseudoelastic NiTi based Belleville washer.
84x60mm (300 x 300 DPI)

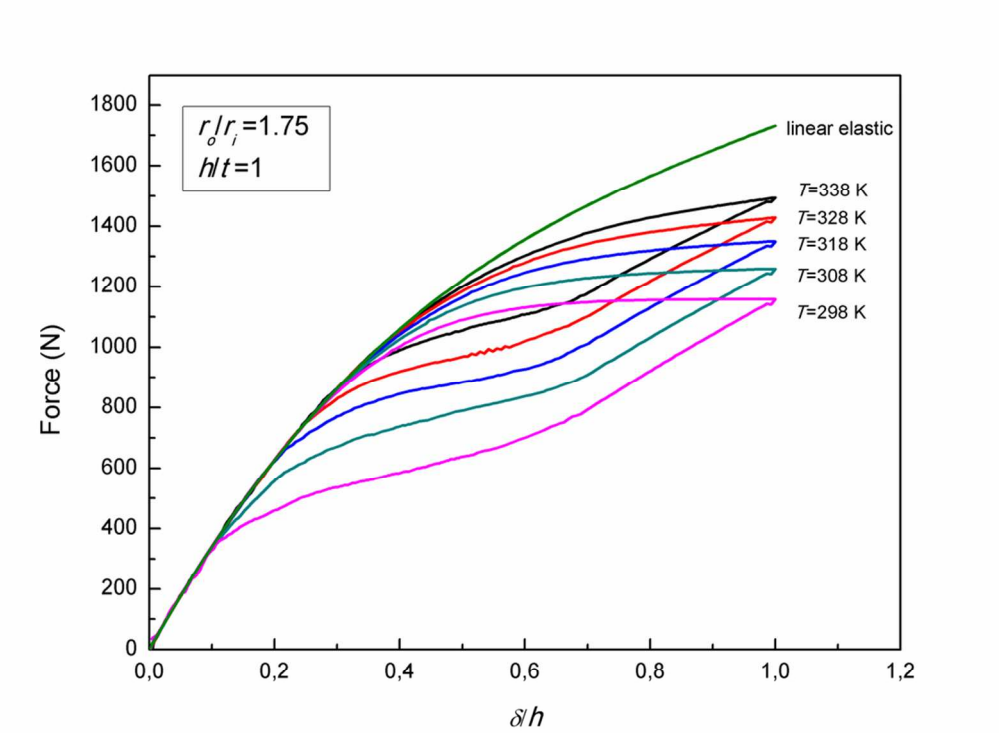

Numerical isothermal force-deflection curves for different values of the temperature for a pseudoelastic NiTi based Belleville washer with ro/ri=1.75 and h/t=1. The curve on the top is related to a washer modeled with a linear elastic material.
91x70mm (300 x 300 DPI)

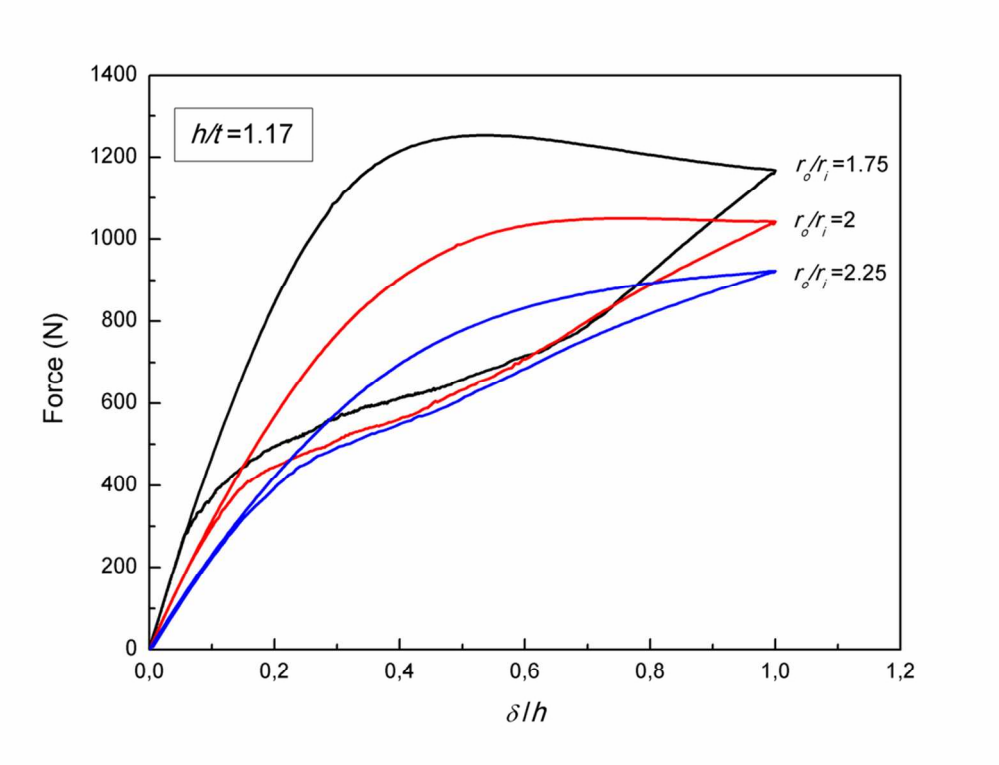

Isothermal force-deflection curves (T=298 K) for a pseudoelastic NiTi based Belleville washer with h/t=1.17 and different values of ro/ri.
91x70mm (300 x 300 DPI)

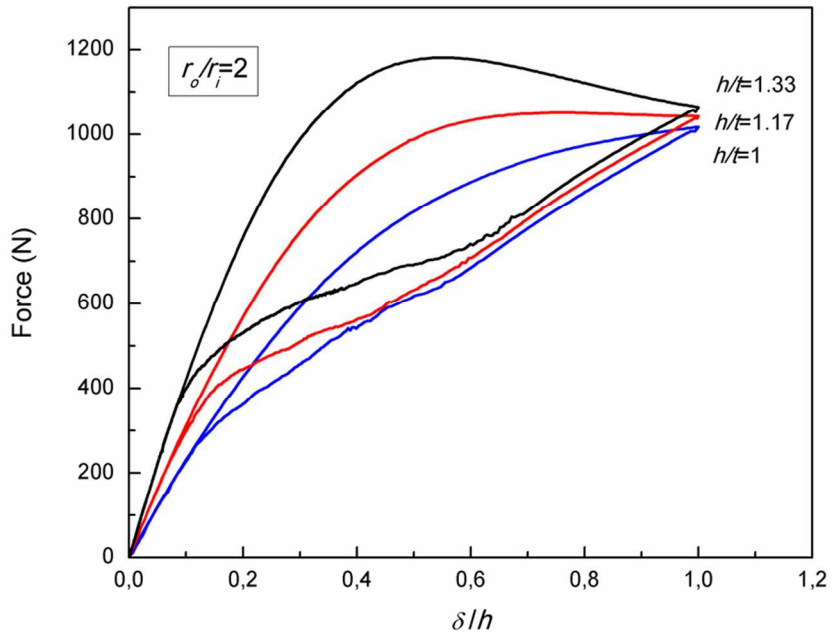

Isothermal force-deflection curves (T=298 K) for a pseudoelastic NiTi based Belleville washer with ro/ri =2 and different values of h/t.
91x70mm (300 x 300 DPI)

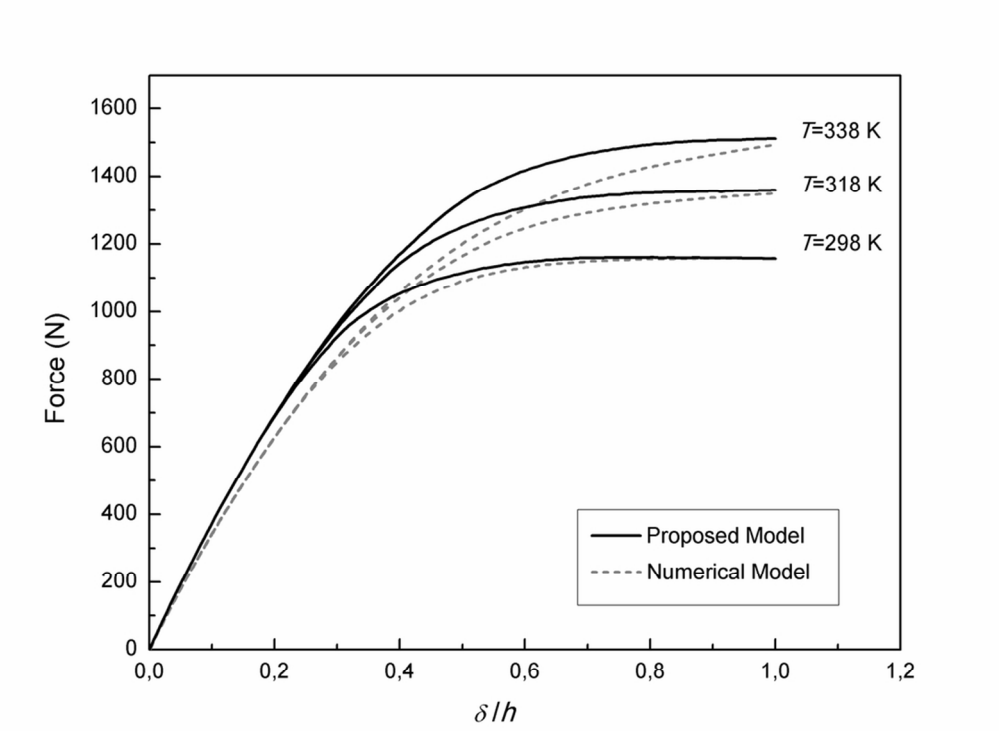

Comparison between the analytical and numerical load-deflection response for a pseudoelastic NiTi based Belleville washer for different testing temperatures. Disk geometry: ro/ri=1.75, h/t=1.
91x70mm (300 x 300 DPI)

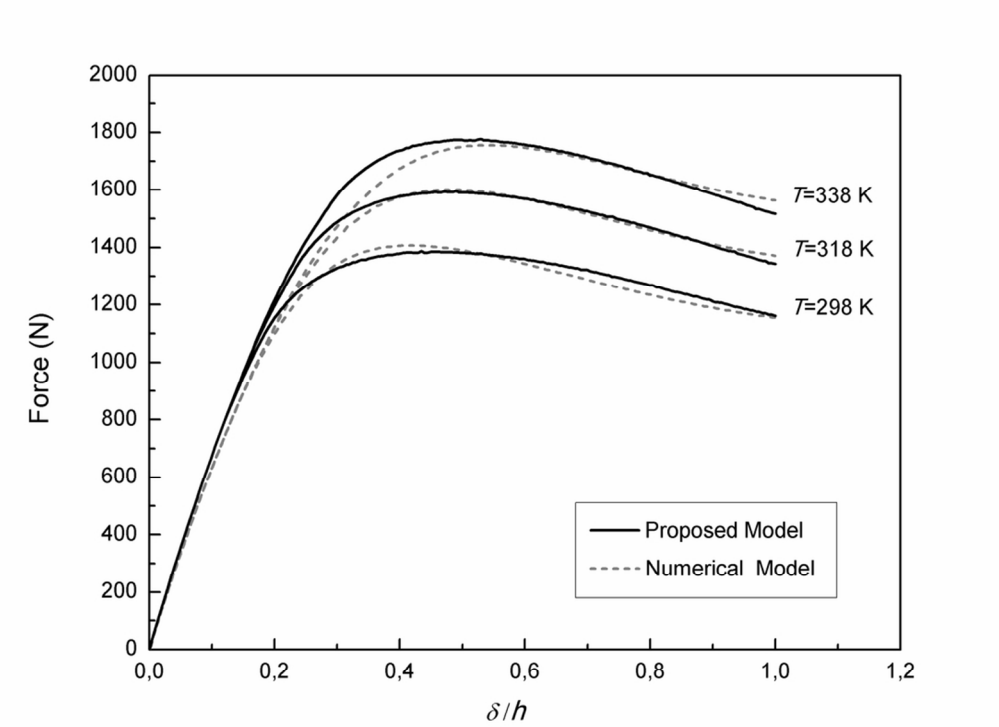

Comparison between the analytical and numerical load-deflection response for a pseudoelastic NiTi based Belleville washer for different testing temperatures. Disk geometry: ro/ri=1.75, h/t=1.33.
91x70mm (300 x 300 DPI)

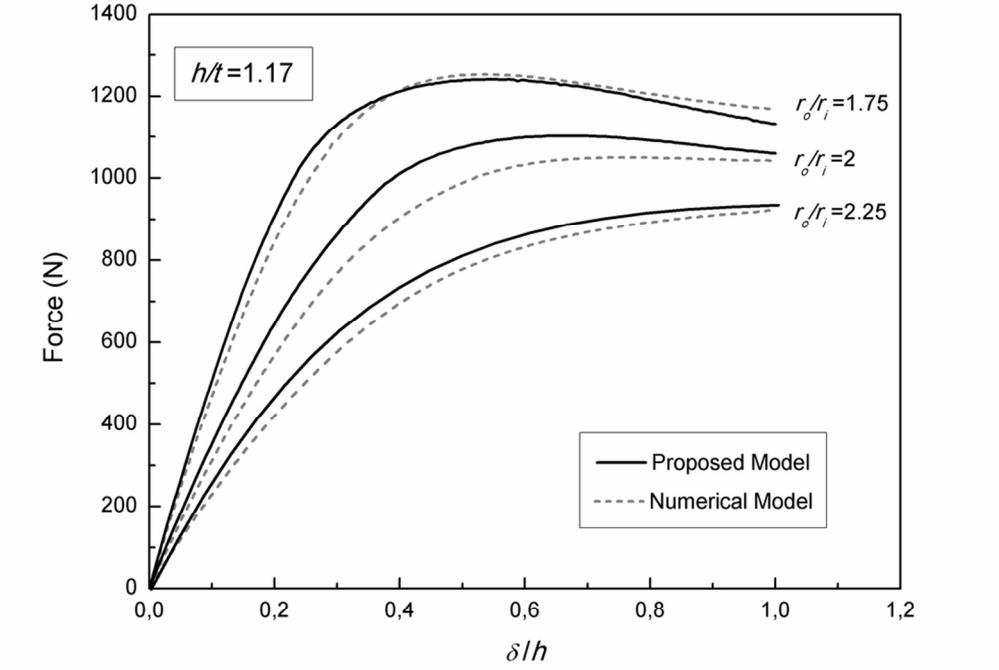

Comparison between the analytical and numerical load-deflection response for a pseudoelastic NiTi based Belleville washer, at room temperature, for different ro/ri ratios and h/t=1.17.
91x70mm (300 x 300 DPI)

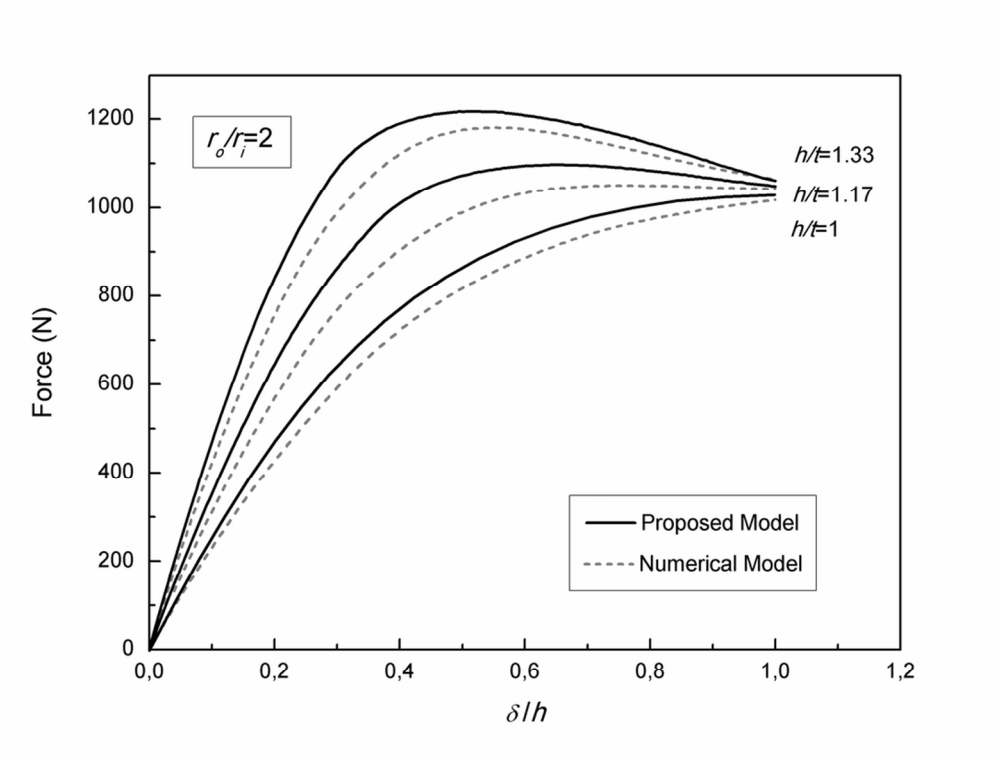

Comparison between the analytical and numerical load-deflection response for a pseudoelastic NiTi based Belleville washer, at room temperature, for different h/t ratios and ro/ri =2.
91x70mm (300 x 300 DPI)

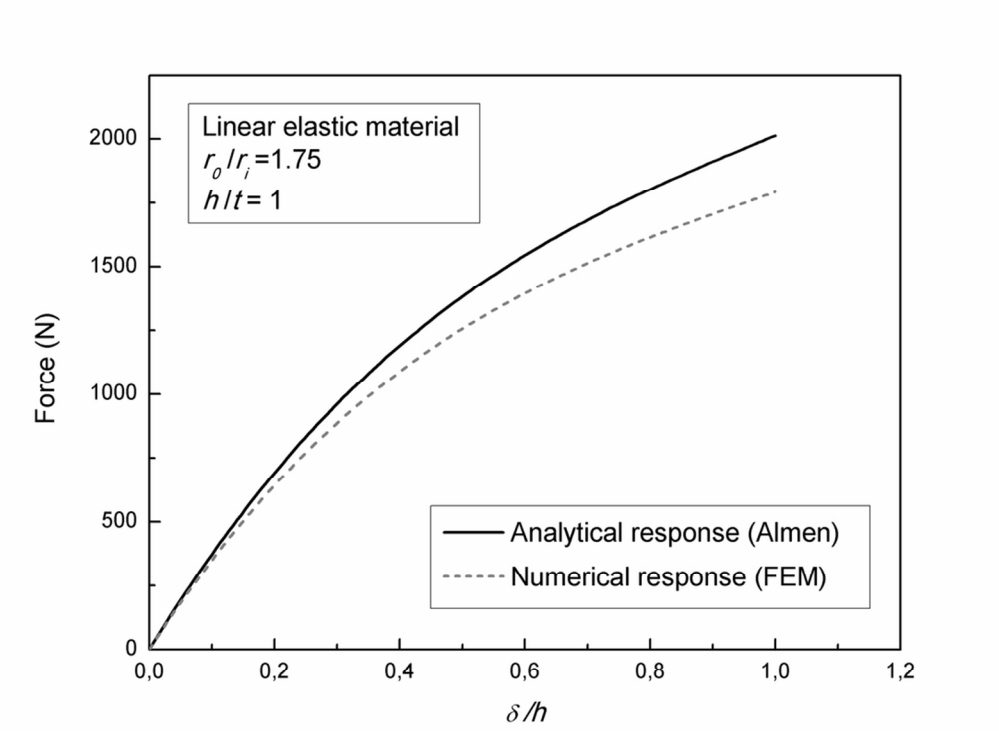

Comparison between the analytical and numerical load-deflection response for a Belleville washer modeled with a linear elastic material, at room temperature. Disk geometry: ro/ri=1.75, h/t=1.
91x70mm (300 x 300 DPI)

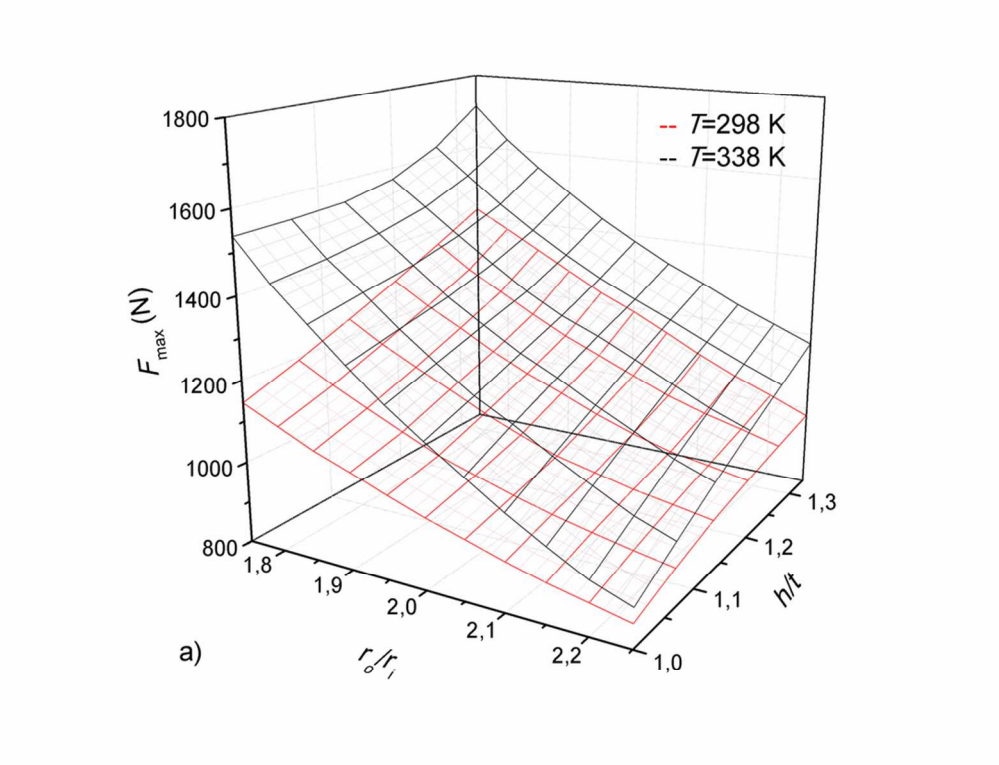

Forces as a function of ro/ri and h/t for two different values of the operating temperature (298 K and 338 K): a) maximum force, Fmax; b) force at the maximum deflection, Fh.
91x70mm (300 x 300 DPI)

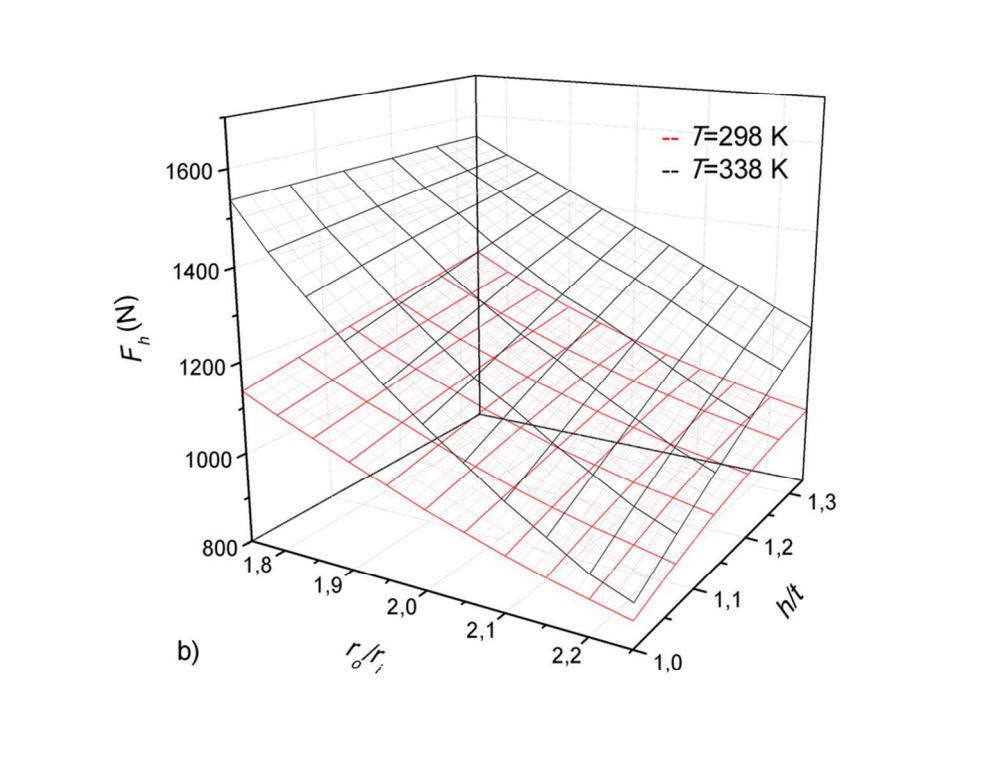

Forces as a function of ro/ri and h/t for two different values of the operating temperature (298 K and 338 K): a) maximum force, Fmax; b) force at the maximum deflection, Fh.
91x70mm (300 x 300 DPI)

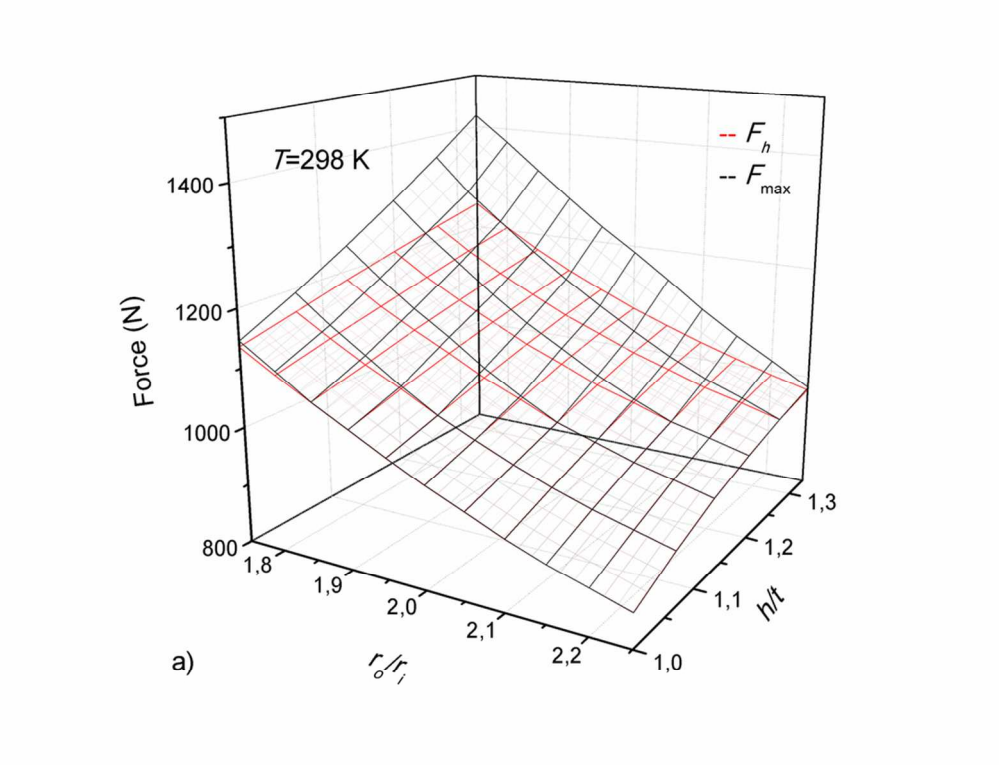

Comparison between the maximum force, Fmax, and the force at the maximum deflection, Fh, as a function of ro/ri and h/t: a) T=298 K; b) T=338 K.
91x70mm (300 x 300 DPI)

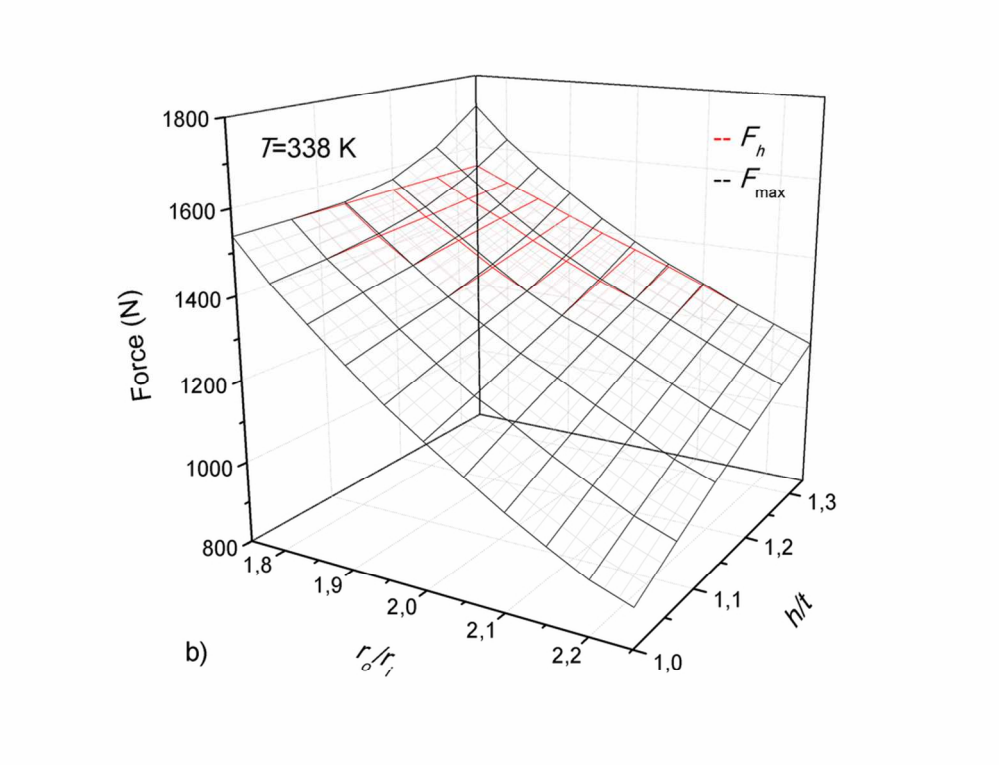

Comparison between the maximum force, Fmax, and the force at the maximum deflection, Fh, as a function of ro/ri and h/t: a) T=298 K; b) T=338 K.
91x70mm (300 x 300 DPI)